A theoretical study of deuteron-induced surrogate reactions

B.V. Carlson[1,a], R. Capote[2], and M. Sin[3]

[1] Instituto Tecnológico de Aeronáutica, DCTA,12.228-900 São José dos Campos, SP, Brazil
[2] NAPC-Nuclear Data Section, International Atomic Energy Agency, 1400 Vienna, Austria
[3] Department of Nuclear Physics, University of Bucharest, PO Box MG-11, 70709 Bucharest-Magurele, Romania

Abstract. We use the zero-range post-form DWBA approximation to calculate deuteron elastic and nonelastic breakup cross sections and estimate the breakup-fusion cross section that could serve as a surrogate for a neutron-induced reaction cross section. We compare the angular momentum dependence of the breakup-fusion compound nucleus formation cross section with that of the corresponding neutron-induced cross section.

1. Introduction

Deuteron-induced reactions, in particular the (d, p) and (d, n) stripping reactions were crucial in the past in determining many aspects of shell structure and in validating the shell model of the nucleus. These stripping reactions have reassumed this role in the last few years as an important tool for determining the structure of exotic nuclei. However, the stripping mechanism is not the only component of a deuteron-induced reaction that can be applied to the study of the nucleus. These reactions have also been considered for many years as substitutes – surrogates – for neutron-induced reactions [1,2]. In this case, competition between elastic and inelastic breakup, absorption of only a neutron or a proton and absorption of the deuteron must be taken into account to determine the formation or not of a compound nucleus. Deuteron breakup-fusion reactions are those in which only a neutron or a proton is absorbed. These form compound nuclei with a wide range of excitation energies and angular momenta and are the cross sections of interest as surrogates to neutron- and proton-induced reactions. Measurements of the ^{238}U(d,pf) cross section, surrogate of the ^{238}U(n,f) cross section, have been performed recently[3–5]. A theoretical estimate of this cross section requires the cross section for deuteron breakup – neutron fusion with the target. We estimate this by the nonelastic breakup cross section and compare its angular momentum dependence with the corresponding neutron-induced CN formation cross sections.

2. The elastic, nonelastic and breakup-fusion cross sections

A reasonable theoretical description of elastic deuteron breakup was developed and applied to a multitude of experimental data almost forty years ago by G. Baur and collaborators [6,7]. The double-differential inelastic breakup cross section can be written in terms of its T-matrix element as

$$\frac{d^6\sigma^{ebu}}{dk_p^3 dk_n^3} = \frac{2\pi}{\hbar v_d}\frac{1}{(2\pi)^6}\left|T(\vec{k}_p, \vec{k}_n; \vec{k}_d)\right|^2 \times \delta(E_d + \varepsilon_d - E_p - E_n) \quad (1)$$

where $\vec{k}_n$ and $\vec{k}_p$ are the final neutron and proton momenta, respectively, $\vec{k}_d$ is the initial deuteron momentum and the sum of neutron and proton final kinetic energies is constrained to the sum of the initial deuteron kinetic energy and its binding energy by the δ-function. The T-matrix element can be well approximated by the post-form of the DWBA matrix element,

$$T(\vec{k}_p, \vec{k}_n; \vec{k}_d) = \left\langle \tilde{\psi}_p^{(-)}(\vec{k}_p, \vec{r}_p)\tilde{\psi}_n^{(-)}(\vec{k}_n, \vec{r}_n) \times \left|v_{pn}(\vec{r})\right| \psi_d^{(+)}(\vec{k}_d, \vec{R})\phi_d(\vec{r})\right\rangle , \quad (2)$$

which, in turn, can be well-approximated within the zero-range DWBA approximation by including corrections for finite-range effects and nonlocality [8,9].

To calculate the nonelastic breakup cross section, one first analyzes the inclusive double differential breakup cross section, here given for the proton, again in the post-form of the DWBA. The initial state of the target is its ground state, Φ_A, but the final neutron-target state, ψ_{nA}^c, can be any composite state allowed by energy and angular momentum conservation,

$$\frac{d^3\sigma}{dk_p^3} = \frac{2\pi}{\hbar v_d}\frac{1}{(2\pi)^3} \times \sum_c \left|\left\langle \tilde{\psi}_p^{(-)}(\vec{k}_p, \vec{r}_p)\psi_{nA}^c \times \left|v_{pn}(\vec{r})\right| \psi_d^{(+)}(\vec{k}_d, \vec{R})\phi_d(\vec{r})\Phi_A\right\rangle\right|^2 \times \delta(E_d + \varepsilon_d - E_p - E_{nA}^c) . \quad (3)$$

This can be separated into an elastic and nonelastic part [10,11], denoted here by *ebu* for elastic breakup and

[a] e-mail: brett@ita.br

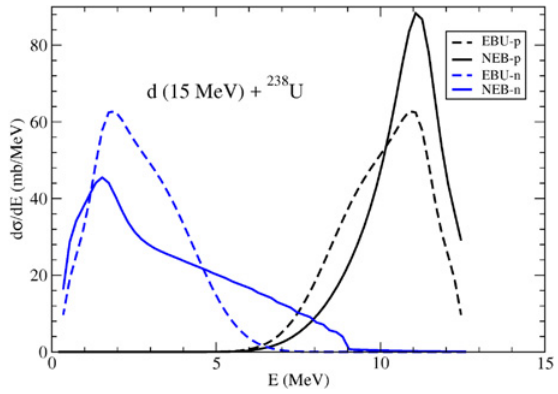

Figure 1. Direct proton and neutron emission spectra due to the elastic and nonelastic breakup of 15 MeV deuterons incident on ^{238}U.

neb for nonelastic breakup, as

$$\frac{d^3\sigma}{dk_p^3} = \frac{d^3\sigma^{ebu}}{dk_p^3} + \frac{d^3\sigma^{neb}}{dk_p^3}. \tag{4}$$

The contribution due to elastic breakup is the double differential elastic breakup cross section of Eq. (1) integrated over the neutron momentum. The nonelastic breakup cross section takes the form of an expectation value of the imaginary part of the optical potential,

$$\frac{d^3\sigma^{neb}}{dk_p^3} = -\frac{2}{\hbar v_d}\frac{1}{(2\pi)^3}\left\langle \Psi_n(\vec{k}_p, \vec{r}_n; \vec{k}_d) \right. \\ \left. \times \left|W_n\left(\vec{r}_n\right)\right| \Psi_n(\vec{k}_p, \vec{r}_n; \vec{k}_d)\right\rangle, \tag{5}$$

where the effective neutron wave function is given by

$$\left|\Psi_n(\vec{k}_p, \vec{r}_n; \vec{k}_d)\right\rangle = \left(\tilde{\psi}_p^{(-)}(\vec{k}_p, \vec{r}_p) G_n^{(+)}\right. \\ \left. \times \left(\vec{r}_n, \vec{r}_n{}'\right) \left|v_{pn}(\vec{r})\right| \psi_d^{(+)}(\vec{k}_d, \vec{R})\phi_d(\vec{r})\right\rangle. \tag{6}$$

The structure of this cross section suggests a simple interpretation in which the deuteron first breaks up, after which the neutron propagates before being absorbed by the nucleus, while the proton is emitted. However, the expression from which it is derived, Eq. (4), describes a one step process.

To perform numerical calculations, the wave functions and matrix elements are expanded in partial waves. The deuteron breakup – neutron fusion cross sections at a given value of the neutron orbital angular momentum and kinetic energy are estimated by summing the nonelastic breakup proton emission partial wave cross sections over the possible values of the deuteron and proton angular momenta. The deuteron breakup – proton fusion cross sections are calculated in similar manner as a sum of the appropriate partial wave cross sections over the deuteron and neutron angular momenta. By taking the breakup fusion cross sections to be the nonelastic ones, we neglect the effects of inelastic scattering and of other direct reaction channels, such as pickup reactions.

In the calculations, we have used the Koning-Delaroche global optical potentials [12] in the proton and neutron channels and the potential of Ref. [13] to describe the deuteron scattering. The elastic breakup matrix

```
* Elastic d breakup cross section                    191.850    mb
* Inelastic d breakup n emission cross section       132.800    mb
* Inelastic d breakup p emission cross section       231.730    mb
* Pre-equilibrium emission cross section            112.663    mb
* Break-up cross section                            0.00000    mb
* Transfer cross section (pick-up/stripping)        23.2089    mb
* TRUE CN formation (after dir. + preeq. emiss.)    188.115    mb
* Fission cross section                             267.534    mb
```

Figure 2. Cross section summary from EMPIRE-3 for 15 MeV deuterons incident on ^{238}U.

```
Fission cross sections (mb)  Total =  267.53 mb

 Z / N    147     146     145     144     143     142
  93     12.77   73.66  150.95    0.26    0.00    0.00
  92     29.34    0.51    0.00    0.00    0.00    0.00
  91      0.00    0.00    0.04    0.00    0.00    0.00


 Initial populations (mb)

 Z / N    147     146     145     144     143     142
  93    880.37  420.42  307.34   88.69    0.00    0.00
  92    236.73  395.46    5.32    0.01    0.00    0.00
  91      0.00    0.00    8.32    0.71    0.00    0.22


Production cross sections (mb) :  Total =  612.67 mb

 Z / N    147     146     145     144     143     142
  93      0.00   35.29   67.70   88.21    0.00    0.00
  92     12.73  394.93    5.31    0.01    0.00    0.00
  91      0.00    0.00    7.56    0.71    0.00    0.22
```

Figure 3. Initial populations, fission and production cross sections from EMPIRE-3 for 15 MeV deuterons incident on ^{238}U.

elements, which are closely related to the nonelastic matrix elements through the breakup wave functions, are only conditionally convergent. A simple brute force application of standard integration methods requires integrating to radii of the order of a nanometer, which can be reduced to radii of the order of picometers by using asymptotic expansions of the Coulomb wave functions to approximate the integral in the external region analytically. We have found the most efficient means of performing the integrals to be their extension to the complex plane [14], in which case the numerical integration can usually be limited to at most several hundreds of fm.

Inclusive elastic and nonelastic (d, p) and (d, n) breakup cross sections have been calculated recently by our group in the post form, as well as by others, using both the prior and post forms of the DWBA [15–18]. The results of the various groups have been found to be quite consistent.

In Fig. 1, we show the elastic and nonelastic neutron and proton breakup spectra for 15 MeV deuterons incident on ^{238}U. The elastic spectra are symmetric about the midpoint energy, due to the fact that the two particles share the kinetic energy remaining after breakup. However, because of the low incident energy and the high charge of the target, the two peaks are widely separated. A simple classical argument, based on the fact that the proton emitted after breakup reaccelerates while the neutron does not, places the two peaks at

$$E_{n,peak} \approx \frac{1}{2}\left(E_d - \frac{Ze^2}{R_{ebu}} - \varepsilon_d\right) \\ E_{p,peak} \approx \frac{1}{2}\left(E_d + \frac{Ze^2}{R_{ebu}} - \varepsilon_d\right), \tag{7}$$

where E_d is the deuteron energy, ε_d the deuteron binding energy, Z the target charge and R_{ebu} the average breakup

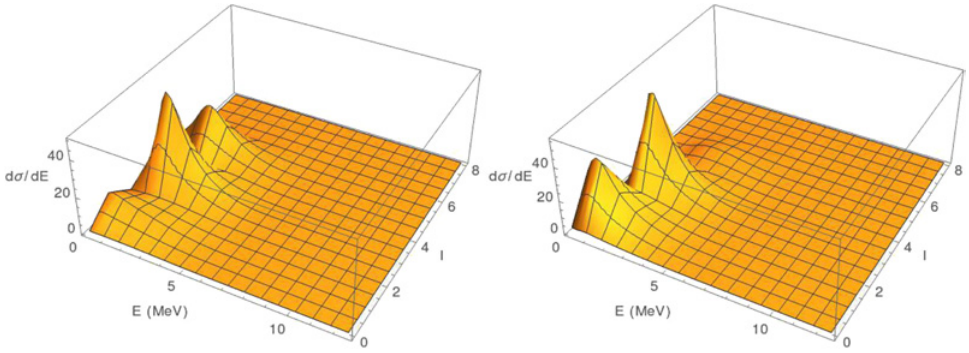

Figure 4. (a) Energy - angular momentum distribution of the (d, p) differential CN formation cross section for 15 MeV deuterons incident on ^{238}U. (b) Renormalized partial wave reaction cross section for neutrons incident on ^{238}U.

radius. In this case, we estimate an average breakup radius of $R_{ebu} \approx 14{,}7$ fm, far outside the ^{238}U radius of about 7,5 fm.

The nonelastic neutron and proton breakup spectra in Fig. 1 are also sharply peaked and somewhat similar in form to the elastic breakup spectra. However, here the proton emission spectrum has about twice the amplitude of the neutron one. This is consistent with the intuitive idea that a neutron will be more easily absorbed (and a proton emitted) than a proton will be absorbed (with a neutron emitted), when the target is highly charged. However, this is not always the case at higher energies [17]. We also note from the high energy peak of the nonelastic proton breakup spectrum that the associated absorbed neutron has a very low average energy kinetic energy of about 1.8 MeV. In contrast, the absorbed proton associated with an emitted nonelastic neutron has an average kinetic energy of about 11 MeV.

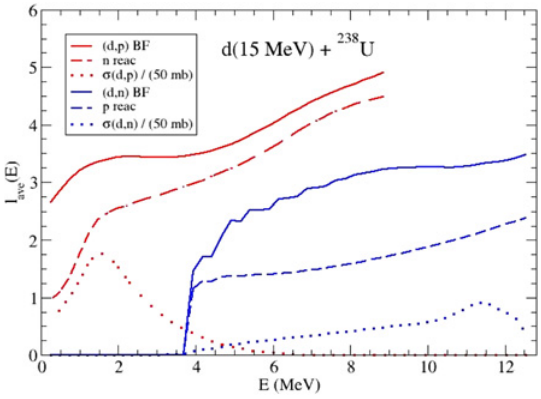

Figure 5. Average angular momentum as a function of energy of the inclusive (d, p) and neutron reaction cross sections (in red). The scaled (d, p) differential cross section, $\sigma(d, p)/$ (50 mb), is shown as a red dotted line. The corresponding (d, n) and proton reaction cross sections are shown in blue.

3. A more complete description of deuteron-induced reactions

A complete description of a deuteron-induced reaction would require taking into account other direct reactions and, most importantly, the formation of the compound nuclei due to deuteron absorption as well as from the neutron absorption or proton absorption of breakup-fusion. We will not take into account any other direct reactions here. Deuteron absorption by the target forms a compound nucleus distributed over a range of angular momentum states, but with a well-defined excitation energy, determined by the initial deuteron energy. The breakup-fusion reactions form two other compound nuclei (the compound nucleus formed by deuteron absorption minus a proton or a neutron) with a fairly wide distribution in both excitation energy as well as angular momentum. These distributions can be included in a nuclear reaction code and the subsequent decay of the compound nuclei can be calculated. We have integrated the deuteron elastic breakup and breakup-fusion into the EMPIRE-3 reaction code[19]. At the moment, we take the breakup-fusion cross sections to be the nonelastic breakup ones, thus neglecting the effects of inelastic breakup, and do not take into account pre-equilibrium emission from the breakup-fusion nuclei.

Cross sections taken from the EMPIRE-3 output for the case of 15 MeV deuterons incident on ^{238}U are shown in Figs. 2 and 3. In Fig. 2, we see that, of the total reaction cross section of 880 mb (given as the initial population of ^{240}Np in Fig. 3), 192 mb correspond to elastic breakup. The breakup-fusion neutron emission, leading to production of the ^{239}Np compound nucleus, has a cross section of 133 mb, while the breakup-fusion proton emission, leading to the ^{239}U compound nucleus has a cross section of 232 mb. After taking into account pre-equilibrium emission, which in this case is principally neutron emission yielding ^{239}Np, the ^{240}Np compound nucleus formation cross section has been reduced to only 188 mb, less than 25% of the total reaction cross section.

In Fig. 3, we show the initial populations, production and fission cross sections for each of the nuclei populated in the 15 MeV deuteron-induced reaction on ^{238}U. The initial population of interest as a surrogate for a neutron-induced reaction is the ^{239}U population of 237 mb, coming mostly from the neutron absorption of 232 mb from the breakup-fusion reaction. The large initial population of 395 mb of the neighboring ^{238}U arises from the elastic component of the breakup reaction (192 mb) and neutron emission from ^{238}U. The initial population of the ^{239}Np is also large, due to the proton absorption of 133mb from the breakup-fusion reaction as well as pre-equilibrium and equilibirum neutron emission from ^{240}Np. The statistical neutron emission cascade continues beyond ^{239}Np, producing a reasonably large initial population of 307 mb for the ^{238}Np nucleus and a smaller initial population of 89 mb for ^{237}Np.

If we now look at the fission and production cross sections for the surrogate nucleus ^{239}U, we find both to be quite small. The production cross section is actually greatly underestimated, as our calculation does not take into account stripping to bound states. The small ^{239}U fission cross section of 29 mb is due to the low average energy of the absorbed neutrons, as deduced above from Fig. 1. We estimated the average kinetic energy of the absorbed neutrons to be about 1.8 MeV while the kinetic energy necessary for fission of ^{239}U is about 1.5 MeV. Thus, the initial ^{239}U population decays for the most part by neutron emission. We note that the production cross section of ^{238}U is almost equal to its initial population, consisting of ^{238}U in its ground state, from the elastic breakup process, and in low-excited states resulting from already low-energy neutron emission from ^{239}U.

4. *(d,p)* breakup-fusion as a surrogate neutron-induced reaction

To better compare the neutron reaction cross section with the nonelastic (d, p) breakup cross section, shown in the left panel of Fig. 4 as a function of neutron energy and orbital angular momentum for a deuteron energy of 15 MeV, we have renormalized the former so as to reproduce the angular momentum summed nonelastic (d, p) cross section as a function of the neutron energy,

$$\frac{d\tilde{\sigma}_n}{dE}(E, l) = \frac{d\sigma_{(d,p)}}{dE}\frac{\sigma_n(E, l)}{\sigma_n(E)} \tag{8}$$

The renormalized neutron reaction cross section is shown in the right-hand panel of Fig. 4. We immediately observe the greater extension in angular momentum of the inclusive nonelastic (d, p) cross section.

To quantify the difference, we compare the average angular momenta of the distributions as a function of the neutron energy E, shown by the red curves in Fig. 5. We observe that the difference in average angular momentum of the (d, p) and neutron reaction cross sections is largest at low neutron energy, but is still about one unit of angular momentum in the region of the energy peak of the (d, p) reaction. A similar conclusion holds for the (d, n) reaction and a proton-induced one, as can be seen by comparing the blue curves in the figure.

We thus find that a (d, p) reaction typically furnishes more angular momentum to the compound nucleus than a neutron-induced reaction at the same neutron energy. This difference limits the extent to which the (d, p) reaction can substitute a neutron-induced one. However, it also opens the possibility of studying nuclei over a wider range of initial populations.

BVC acknowledges partial support from the Brazilian funding agencies FAPESP (Project 2009/00069-5) and the CNPq (Project 306692/2013-9) as well as from the International Atomic Energy Agency (Research Contract 17740).

References

[1] H.C. Britt, J.D. Cramer, Phys. Rev. C **2**, 1758 (1970)
[2] J.E. Escher, J.T. Burke, F.S. Dietrich, N.D. Scielzo, I.J. Thompson, W. Younes, Rev. Mod. Phys. **84**, 353 (2012)
[3] Q. Ducasse et al., EPJ Web of Conferences **62**, 08002 (2013)
[4] P. Marini et al., CERN Proceedings-2015-001, 195 (2015)
[5] Q. Ducasse et al., Phys. Rev C **94**, 024614 (2016)
[6] G. Baur, D. Trautmann, Phys. Rep. **25**, 293 (1976)
[7] G. Baur, F. Rösel, D. Trautmann, R. Shyam, Phys. Rep. **111**, 333 (1984)
[8] P.J.A. Buttle, L.J.B. Goldfarb, Proc. Phys. Soc. **83**, 701 (1964)
[9] F. Perey, B. Buck, Nucl. Phys. **32**, 353 (1962)
[10] A. Kasano, M. Ichimura, Phys. Lett. **B115**, 81 (1982)
[11] N. Austern, Y. Iseri, M. Kamimura, M. Kawai, G. Rawitscher, M. Yahiro, Phys. Rep. **154**, 125 (1987)
[12] A.J. Koning, J.P. Delaroche, Nucl. Phys. A **713** 231, (2003)
[13] Y. Han, Y. Shi, Q. Shen, Phys. Rev. C **74**, 044615 (2006)
[14] C.M. Vincent, H.T. Fortune, Phys. Rev. C **2**, 782 (1970)
[15] J. Lei, A.M. Moro, Phys. Rev. C **92**, 044616 (2015); Phys. Rev. C **92**, 061602(R) (2015)
[16] G. Potel, F.M. Nunes, I.J. Thompson, Phys. Rev. C **92**, 034611 (2015)
[17] B. V. Carlson, R. Capote, M. Sin, CERN Proceedings-2015-001, 163 (2015)
[18] B.V. Carlson, R. Capote, M. Sin, Few-Body Syst. **57**, 307 (2016)
[19] M. Herman, R. Capote, B.V. Carlson, P. Oblozinský, M. Sin, A. Trkov, H. Wienke, V. Zerkin, NDS **108**, 2655 (2007)